Electronic Supplementary Information

Solvent driven phase transitions of acyclovir – the role of water and solvent polarity

Karol P. Nartowski[1,2,*], Julia Karabin[1], Alexander L. Morritt[2], Maciej Nowak[1], László Fábián[2], Bożena Karolewicz[1], Yaroslav Z. Khimyak[2,*]

[1]Department of Drug Form Technology, Wrocław Medical University, ul. Borowska 211, 50-556 Wrocław, Poland

[2]School of Pharmacy, University of East Anglia, Norwich Research Park, NR4 7TJ Norwich, United Kingdom

e-mail addresses: karol.nartowski@umed.wroc.pl and y.khimyak@uea.ac.uk

Contents of Electronic Supplementary Information:

Contents

Section S1. Thermal stability of ACV form V during dehydration process 2
Section S2. Solvents used in the study 3
Section S3. Dehydration of ACV form V and ACV form VI. 4
Section S4. The Critical water activity determination in MeOH and NNDMF. 5
Section S5. The Critical water activity determination in MeOH and NNDMF. 7
Section S6. Variable temperature FTIR spectra of ACV form I. 8
Section S7. Solid-state NMR studies of ACV polymorphs (ACV form I, ACV form II) and hydrates (ACV form V and ACV form VI) stable at room temperature. 9
Section S8. Temperature induced phase transitions of ACV form I and ACV form V 13
Section S9. Solvent induced phase transitions of ACV form V (3:2 ACV/water hydrate) 15
Section S10. Solvent induced phase transitions of ACV form I (anhydrous form I) 23

Section S1. Thermal stability of ACV form V during dehydration process

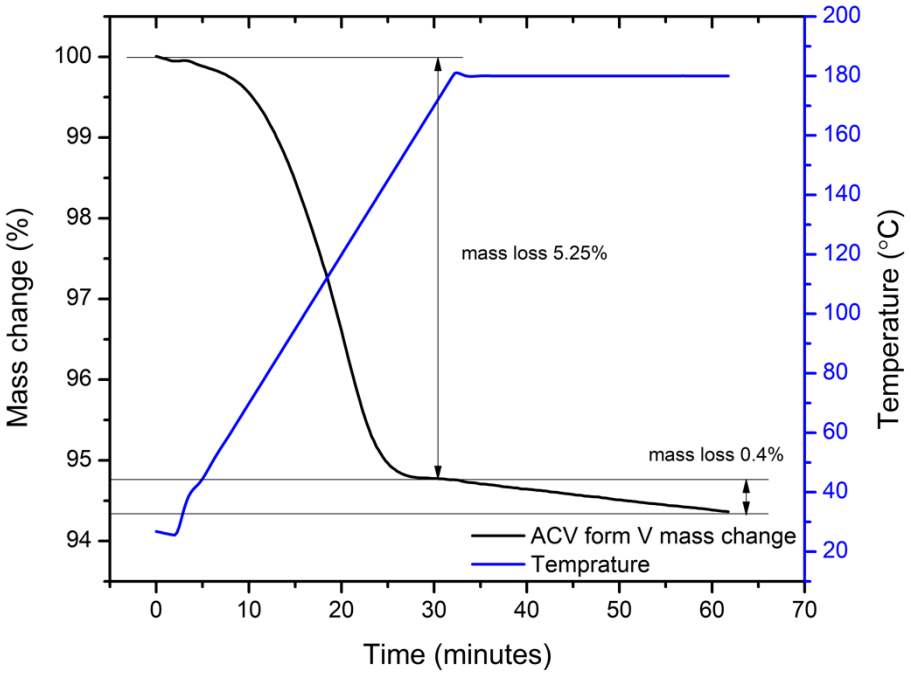

Figure S 1. TGA thermogram of ACV form V heated to 180 °C and stored at 180 °C for 30 minutes.

Acyclovir after storage at 180 °C for 30 minutes lost maximum of 0.4% mass, which indicates the drug was thermally stable during preparation of the material.

Section S2. Solvents used in the study

Table S 1. Properties of the solvents used in the study.

Solvent	Formula	Σα[a]	Σβ[b]	Dielectric constant	Dipole momentum[c]	δD[d]	δP[d]	δH[d]
Water	H_2O	1.17	0.47	78.36	1.87	15.5	16.0	42.3
Methanol	CH_3OH	0.43	0.47	32.61	1.70	14.7	12.3	22.3
Ethanol	C_2H_5OH	0.37	0.48	24.85	1.69	15.8	8.8	19.4
n-Propanol	C_3H_7OH	0.37	0.48	20.52	1.55	16.0	6.8	17.4
Iso-propanol	C_3H_7OH	0.33	0.56	19.26	1.56	15.8	6.1	16.4
n-Butanol	C_4H_9OH	0.37	0.48	17.33	1.66	16.0	5.7	15.8
Acetone	CH_3COCH_3	0.04	0.49	20.49	2.88	15.5	10.4	7.0
Acetonitrile	CH_3CN	0.07	0.32	35.69	3.92	15.3	18.0	6.1
Dimethylformamide	$(CH_3)_2NCHO$	0.00	0.74	37.22	3.82	17.4	13.7	11.3
Dimethyl sulfoxide	CH_3SOCH_3	0.00	0.88	46.83	1.80	18.4	16.4	10.2
Acetic acid	CH_3COOH	0.61	0.44	6.25	1.70	14.5	8.0	13.5
Ethyl acetate	$CH_3COOC_2H_5$	0.00	0.45	5.99	1.78	15.8	5.3	7.2
Toluene	$C_6H_5CH_3$	0.00	0.14	2.37	0.38	18.0	1.4	2.0
Dichloromethane	CH_2Cl_2	0.10	0.05	8.93	1.60	17.0	7.3	7.1
Chloroform	$CHCl_3$	0.15	0.02	4.71	1.04	17.8	3.1	5.7

[a] – Abraham's[1] hydrogen bond acidity (Abraham's notation $\Sigma\alpha_2^H$), [b] – Abraham's[1] hydrogen bond basicity (Abraham's notation $\Sigma\beta_2^H$), [c] – Dipole moment in the unit of Debye; [d] - Hansen solubility parameter values accounting for dispersion forces (δD), dipolar intermolecular forces (δP) and hydrogen bonds between molecules(δH) in the unit of $MPa^{0.5}$S1. Packing of ACV crystal structures: form I, form II, form V (3:2 hydrate), form VI (dihydrate).

Section S3. Dehydration of ACV form V and ACV form VI.

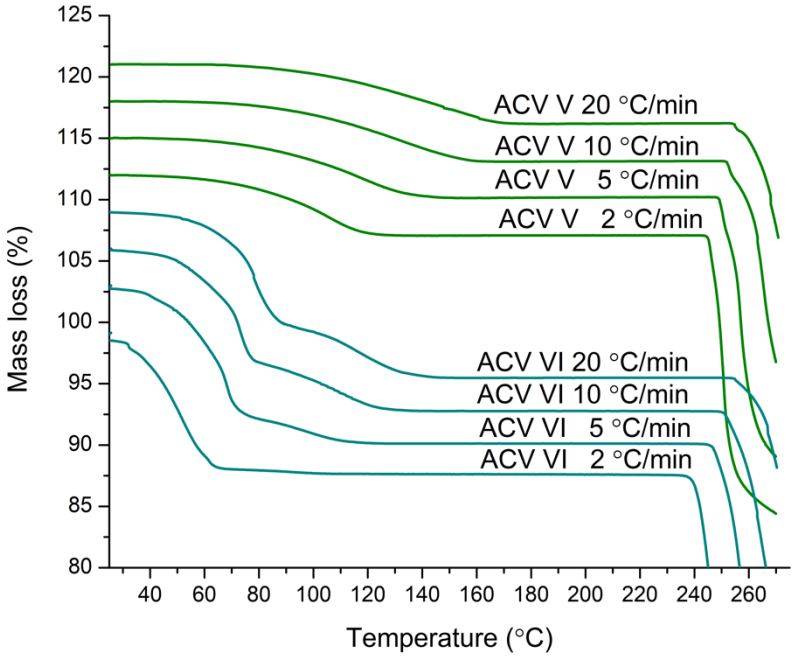

Figure S 2. TGA thermograms of ACV form V and ACV form VI recorded at different heating rates from 2 to 20 °C. Two step dehydration is observed for ACV dihydrate

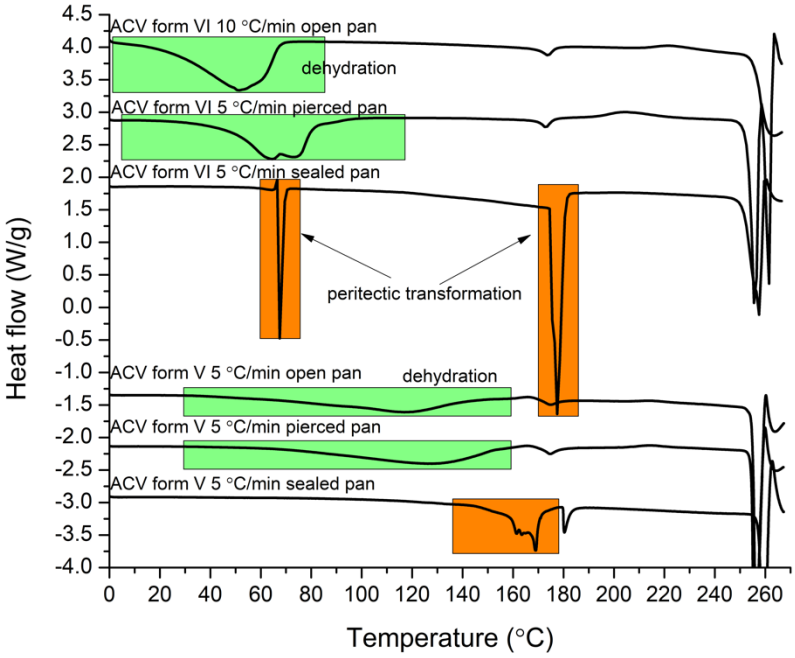

Figure S 3. DSC thermograms of ACV forms V and VI performer using open, pierced and sealed pans. The peritectic dissociation/transformation events are marked in orange while dehydration of both hydrates is marked in green.

Section S4. The Critical water activity determination in MeOH and NNDMF.

The water activity plots in MeOH and NNDMF were prepared using the previously reported data (Figures S2 and S3).[2–5] The slurring of ACV form I in MeOH at different a_w resulted in the formation of form II at $a_w \leq 0.14$ and mixture of form II and form V at $a_w \geq 0.18$ as determined using PXRD (Figure S4 A.). The slurring of ACV form I in NNDMF resulted in formation of form II at a_w in the range from 0.03 to 0.38 (Figure S4B.).

The slurring of ACV form V in MeOH led to recrystallisation to form I at $a_w \leq 0.1$ with traces of ACV dihydrate observed in PXRD patterns while formation of mixture of forms I, V and VI was observed in the a_w range from 0.1 to 0.24. Only ACV form V was detected using PXRD after slurring in the water/MeOH mixture at $a_w = 0.26$. Slurring of ACV form V in NNDMF resulted in formation of form I at $a_w \leq 0.22$ and mixture of ACV forms V and I at $a_w \geq 0.24$. Furthermore, the respective content of ACV form I in the mixture of ACV form V and form I was decreasing with increasing a_w.

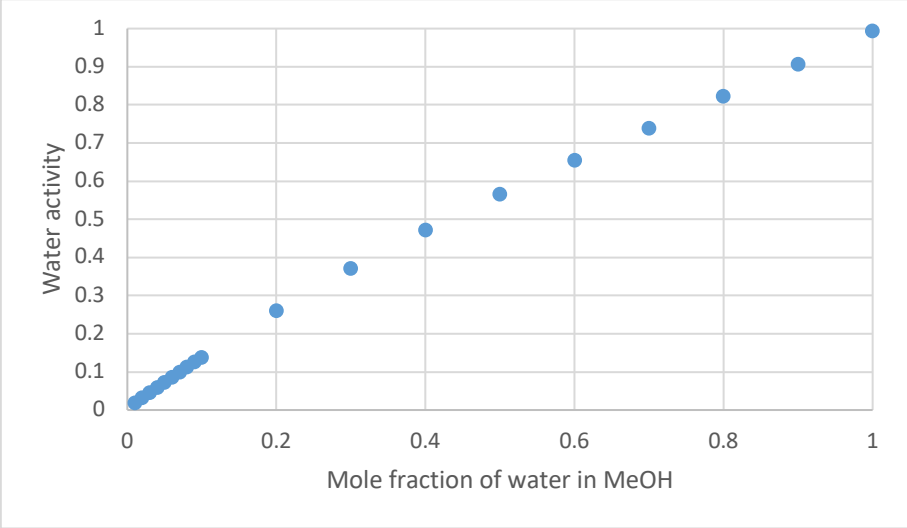

Figure S 4. Water activity at different mole fractions of water in water/methanol and water/NNDMF mixtures at 25 °C. The data extracted from reference.[2]

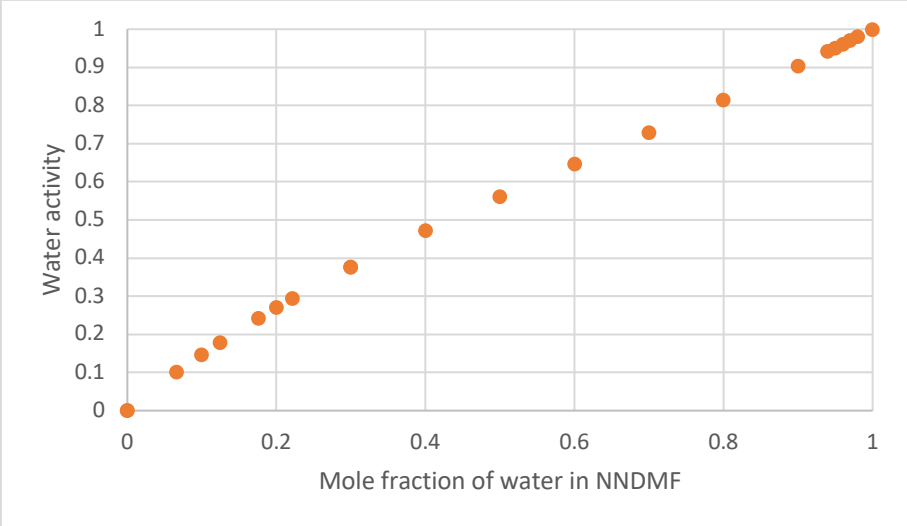

Figure S 5. Water activity at different mole fractions of water in water/methanol and water/NNDMF mixtures at 25 °C. The plot created using equation from ref.[4]

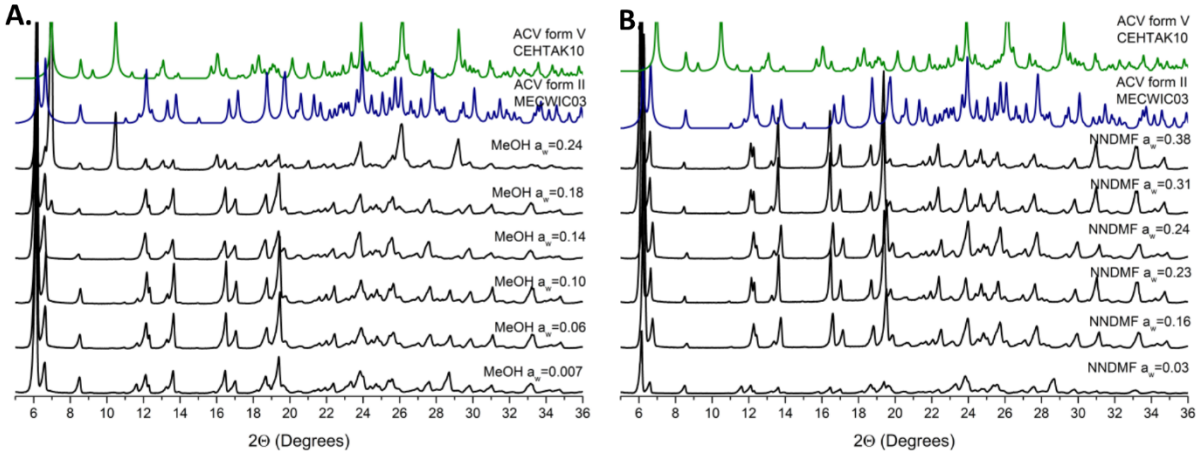

Figure S 6. PXRD patterns of ACV form I in water/methanol (A.) and water/NNDMF (B.) mixtures at different a_w.

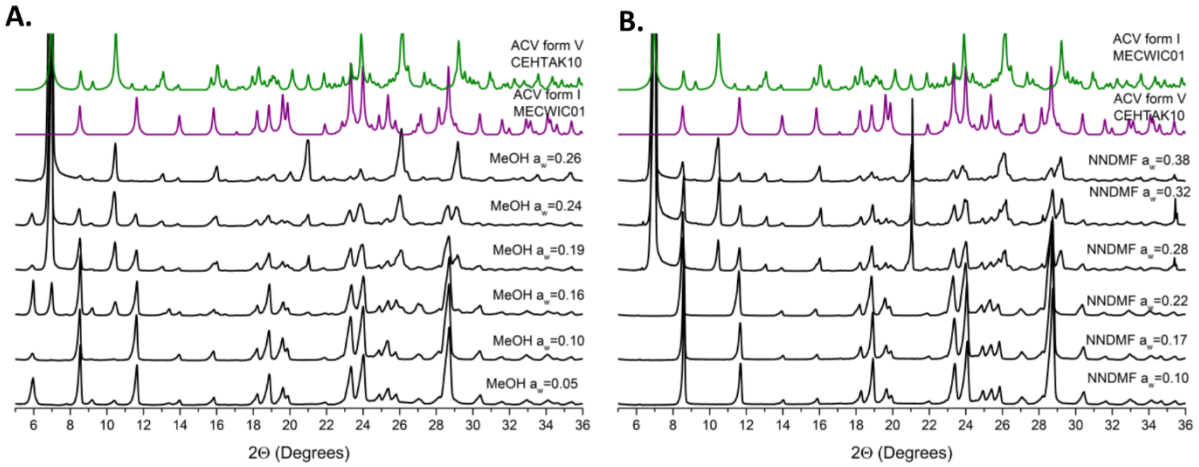

Figure S 7. PXRD patterns of ACV form V in water/methanol (A.) and water/NNDMF (B.) mixtures at different a_w

Section S5. ACV form V seeding and intensive mixing experiments.

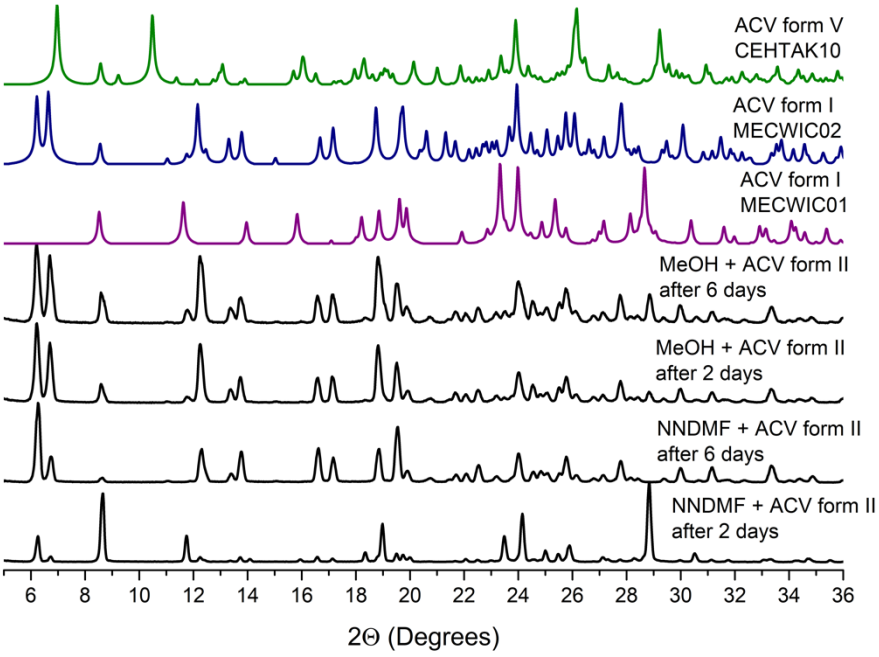

Figure S 8. ACV form V slurried in NNDMF and MeOH with seeds of form II. After 6 days complete conversion is observed in NNDMF and nearly complete in MeOH.

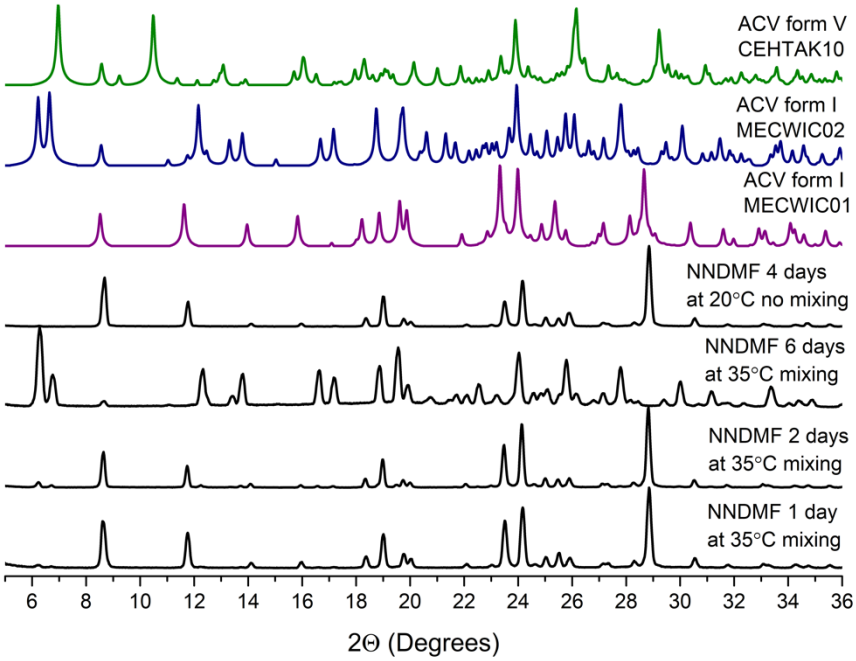

Figure S 9. ACV form V slurried in dry NNDMF at 35 °C and intense mixing. Formation of firstly ACV form I after one day followed by recrystallisation to form II was observed after 6 days. For comparison PXRD pattern of the material obtained in control slurrying experiment at 20 °C with no agitation is shown. Only peaks of form I can be distinguished.

Section S6. Variable temperature FTIR spectra of ACV form I.

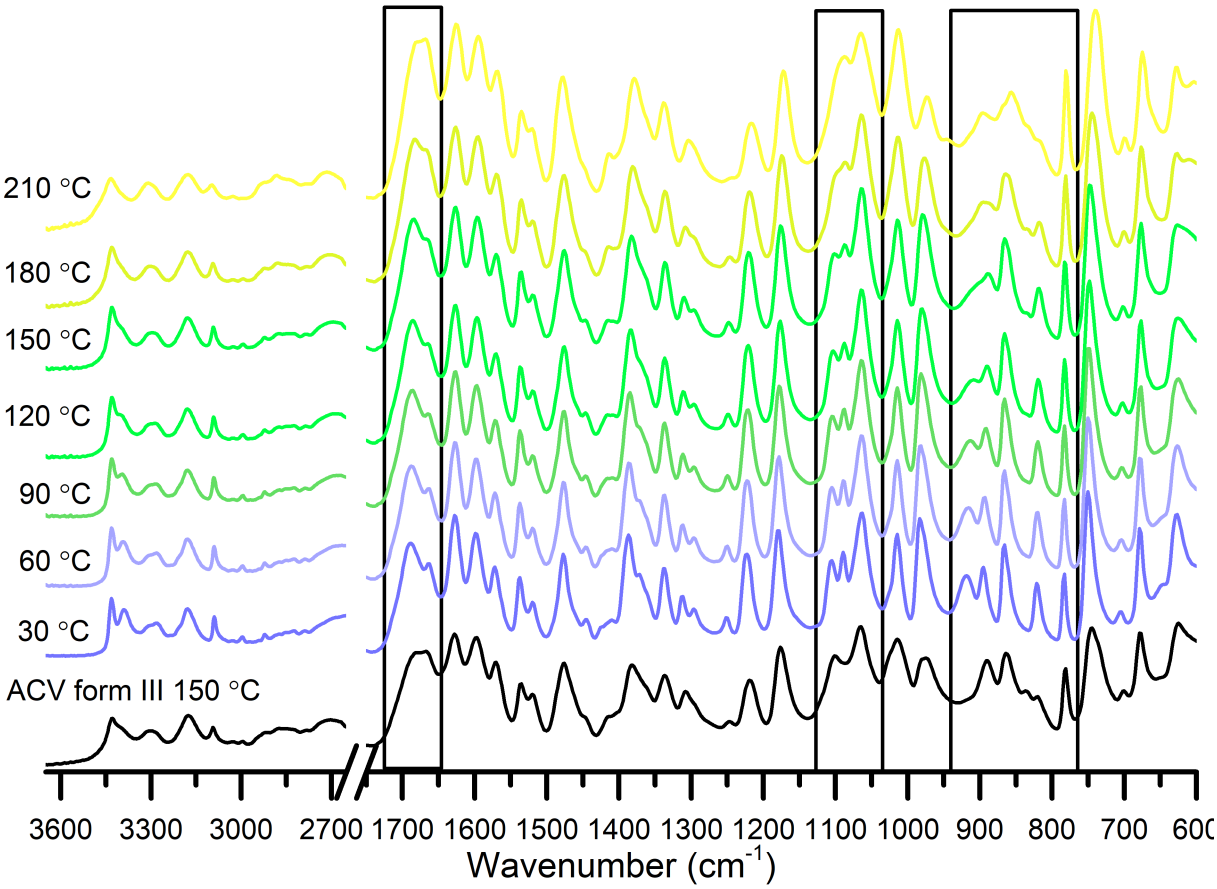

Figure S 10. Variable temperature FTIR spectra of ACV form I as compared to ACV form III recorded at 150 °C. The regions with differences between the ACV form III spectra and ACV form I at high temperatures are highlighted in black frames.

Section S7. Solid-state NMR studies of ACV polymorphs (ACV form I, ACV form II) and hydrates (ACV form V and ACV form VI) stable at room temperature.

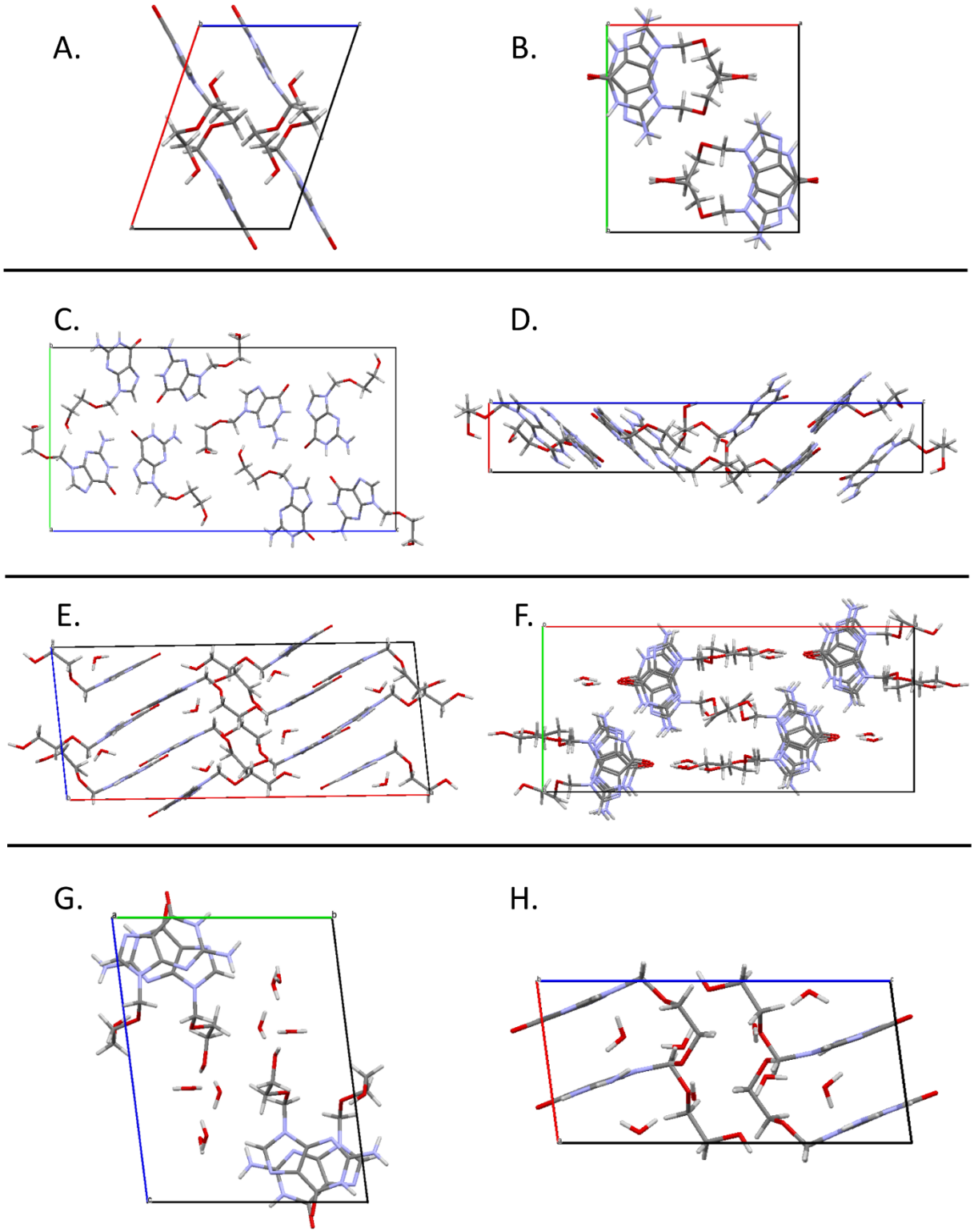

Figure S 11. Packing of ACV form I (A., B., CSD ref. code MECWIC01); form II (C., D., CSD ref. code MECWIC03); form V (E., F, CSD ref. code CEHTAK10); form VI (G., H., CSD ref. code WOZPAE).

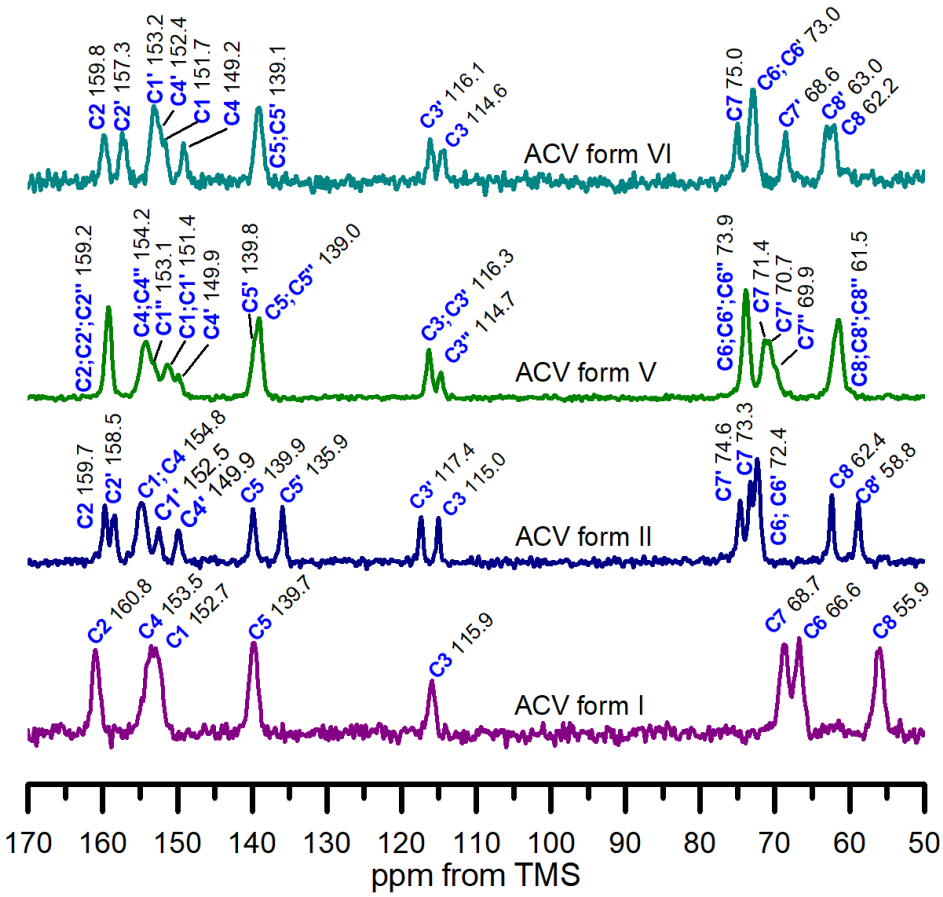

Figure S 12. ^{1}H-^{13}C CP/MAS NMR spectra of ACV forms I, II, V and VI.

As ACV form V has three ACV molecules in the asymmetric unit, 24 peaks can be expected in the ^{1}H-^{13}C CP/MAS solid-state NMR spectrum. The presence of lower number of peaks (15 peaks) in the spectrum is likely due to very similar local environment of ACV carbon atoms in the structure resulting in similar values of ^{13}C chemical shifts. The ^{13}C peaks are grouped in three distinct regions of the spectrum. Carbons C6, C7 and C8 of aliphatic tail of each ACV molecule (e.g. C6, C6', C6'' representing C6 carbon of three distinct ACV molecules in the asymmetric unit) are observed in the spectral region from 60 to 75 ppm. Carbons C8, C8', C8'' of three different ACV molecules appear as a single, slightly broadened peak at 61.5 ppm. Similarly, carbons C6, C6' and C6'' are observed as a sharp peak at 73.9 ppm. Three carbons C7, C7' and C7'' appear as a broad resonance composed of three overlapping peaks at 71.4, 70.7 and 69.9 ppm. Carbons C3 of the purine ring are observed as distinct peaks at 114.7 (C3'') and 116.3 (C3 and C3') ppm while carbons C1, C2, C4 and C5 are grouped in the region from 140 to 160 ppm. Despite of the presence of three distinct molecules in the asymmetric unit, their layered arrangement and similar bonding pattern in the crystal structure may result in very similar electronic environments and in very small distinct differences between the molecules in the ^{1}H-^{13}C CP/MAS NMR spectrum observed as overlapping of the ^{13}C peaks.

The ^{1}H-^{13}C CP/MAS NMR spectrum of ACV form I obtained via dehydrating of form V display significant differences as compared to the starting material (ACV form V). Firstly, there are eight peaks in the spectrum (Z' = 1), which can be assigned to eight carbon atoms of ACV in agreement with crystallographic data. Secondly, the peaks of aliphatic side chain of ACV grouped in high-frequency region of the spectrum display a 5 and 6 ppm up-field shifts of carbons C8, C6 as compared to form V. This may be due to the involvement of carbons of a side chain of ACV form V in hydrogen bonding and short contact interactions with electronegative nuclei and water molecules present in the crystal structure. As water oxygens are more electronegative than carbons (and protons) they tend to polarize the electron clouds of neighboring nuclei towards themselves, which result in a

deshielding effects observed as a peak shift towards lower frequencies. This phenomenon was described in detail by Spiess *et al.* for ciprofloxacin hydrates using a combined application of state of the art solid-state NMR methods and CASTEP caluclations.[6] The ^{13}C peaks of the purine ring of ACV form I undergo only minor changes as compared to the structure of ACV form V. This may reflect planar arrangement of the molecules in both structures and their stabilization via similar hydrogen bonding pattern.

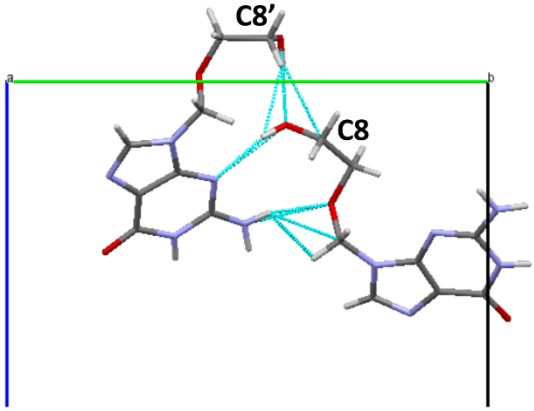

Figure S 13. Hydrogen bonds and short contact interactions involving carbons C8 and C8' in two molecules of ACV in the asymmetric unit of ACV form II.

The presence of two ^{13}C peaks for each carbon atom in the spectrum of ACV form II is consistent with there being two molecules in the asymmetric unit in agreement with crystallographic data. The significant downfield shift of carbon C8 as compared to carbon C8' may be a result of two hydrogen bonds between the hydroxy group at C8 and nitrogen N1 and hydroxy group of second ACV molecule (Figure S3). Further significant downfield shift of 4 ppm of C5 as compared to C5' site may arise due to three short contact interactions of carbon C5 with two carbonyl oxygens and N3 hydrogen of neighbouring molecules.[6] Small chemical shift difference of 1.2 ppm between carbonyls C2 and C2' may be due to hydrogen bonding of carbonyl C2 with amino group hydrogen (N5) and carbonyl C2' with hydrogen at nitrogen N3. Very different arrangement of ACV molecules in the crystal structure of ACV form I and ACV form II may result in different pathways for the phase transitions of these two structures on heating i.e. ACV form I transforms to the high temperature form IV above 180 °C while ACV form II does not undergo any phase change prior melting.

Similarly, to ACV form II, the ACV 1:2 dihydrate (form VI) has two ACV molecules in the asymmetric unit resulting in two peaks per each carbon observed in the ^{1}H-^{13}C CP/MAS spectrum. The unit cell is composed of four ACV molecules with antiparallel arrangement of the purine rings and eight water molecules organized in two channels in close proximity to aliphatic side chain (Figure S1 G, H). The antiparallel arrangement of the purine rings between form VI and form I was used by Terada *et al*. as a possible explanation of water sorption induced phase change of form I to form VI.[7] The significant downfield shift of C6 and C6' peaks in form VI spectrum as compared to form I may be due to short contact interactions of carbon C6 and C6' with electronegative nuclei: nitrogen N4, ether oxygen of the side chain (C6) and water oxygen (C6'). The chemical shift difference of *ca*. 6 ppm between C7 and C7' sites may be a result of carbon C7' facing towards water cannel with four water molecules in close proximity (below ca. 3.5 Å). The two ACV molecules forming asymmetric unit of form VI lead to different hydrogen bonds via carbonyl motif. The carbonyl C2 is involved in three hydrogen bonds between two water molecules and amino group of neighboring ACV, while carbonyl C2' forms two hydrogen bonds with one water molecule and an amino group of neighboring ACV. This may be reflected as a slight upfield shift of C2 carbonyl to 159.7 ppm as compared to 158.5 ppm for C2' carbonyl.

Table S 2. Experimental and CASTEP calculated ^{13}C chemical shifts of ACV forms I, II, V and VI.

Atom	ACV form I		ACV form II		ACV form V		ACV form VI	
	δ_{exp}	δ_{calc}	δ_{exp}	δ_{calc}	δ_{exp}	δ_{calc}	δ_{exp}	δ_{calc}
C2	160.8	160.0	159.7	159.2	159.2	159.5	159.8	159.7
C2'	-	-	158.5	157.7	159.2	159.5	157.4	157.1
C2''	-	-	-	-	159.2	159.3		
C1	153.5	153.5	154.8	154.0	151.4	151.9	151.7	151.4
C1'	-	-	152.5	153.0	151.4	152.3	153.2	152.5
C1''	-	-	-	-	153.1	153.4		
C4	152.7	151.0	154.8	153.5	154.2	153.8	149.2	150.9
C4'	-	-	149.9	150.4	149.9	151.6	152.4	152.4
C4''	-	-	-	-	154.2	154.2		
C5	139.7	141.4	139.9	141.8	139.0	141.3	139.1	143.0
C5'	-	-	135.9	138.2	139.8	141.2	139.1	141.4
C5''	-	-	-	-	139.0	140.9		
C3	115.9	119.1	115.0	118.1	116.3	120.4	114.6	118.3
C3'	-	-	117.4	121.1	116.3	120.1	116.1	118.9
C3''	-	-	-	-	114.7	118.9		
C7	68.7	69.9	73.3	77.0	73.9	76.1	75.0	77.9
C7'	-	-	74.6	77.5	70.7	74.6	68.8	73.1
C7''	-	-	-	-	69.9	74.0		
C6	66.6	67.7	72.4	75.0	73.9	77.6	73.0	76.9
C6'	-	-	72.4	74.2	73.9	77.6	73.0	77.0
C6''	-	-	-	-	71.4	76.8		
C8	55.9	55.7	62.4	63.6	61.5	65.6	62.2	66.7
C8'	-	-	58.8	60.0	61.5	65.8	63.0	66.1
C8''	-	-	-	-	61.5	66.1		

Section S8. Temperature induced phase transitions of ACV form I and ACV form V

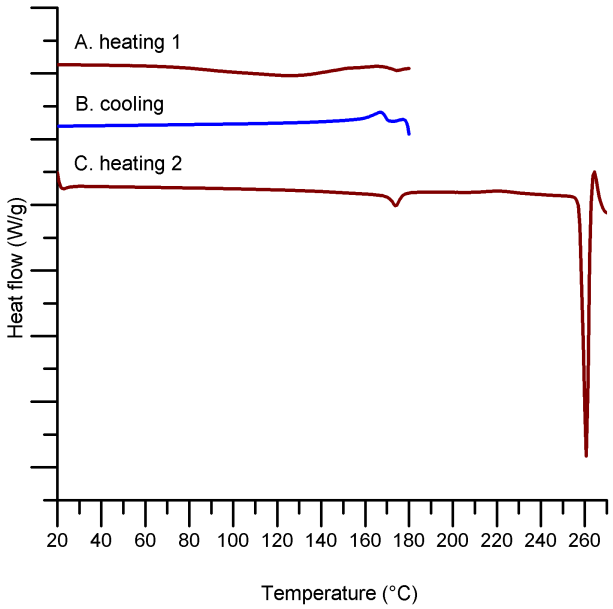

Figure S 14. DSC thermograms of ACV form V showing reversible transition at ca. 170 °C: A. First heating from 20.0 to 180.0 °C; B. Cooling from 180.0 to 20.0 °C; C. Second heating from 20.0 to 280.0 °C.

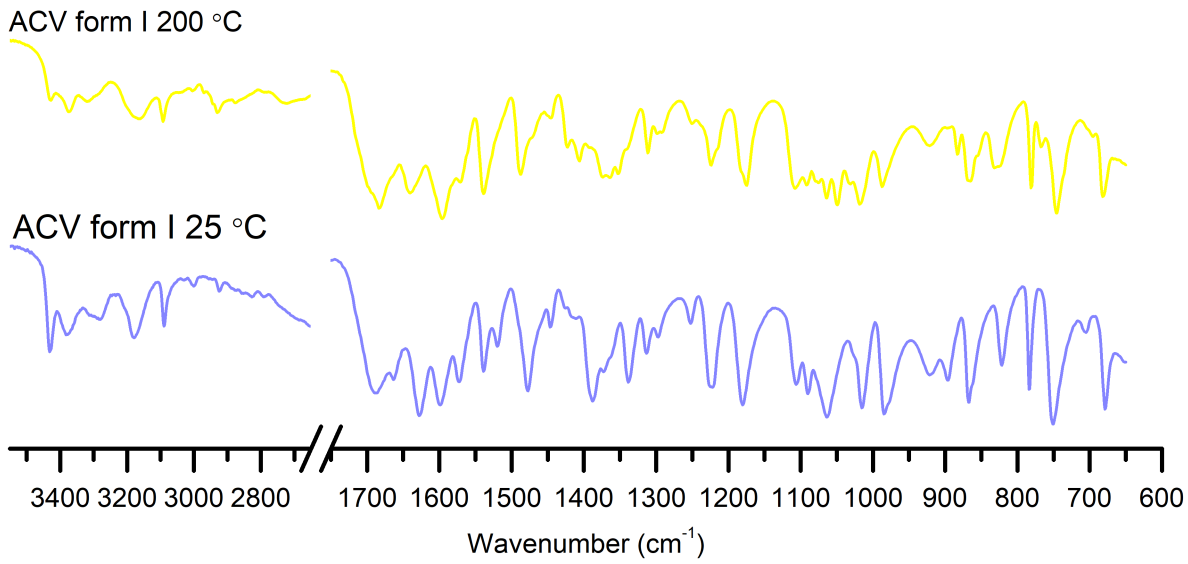

Figure S 15. FTIR spectra of ACV form I at 25 °C and 200 °C showing transition to ACV form IV above 170 °C.

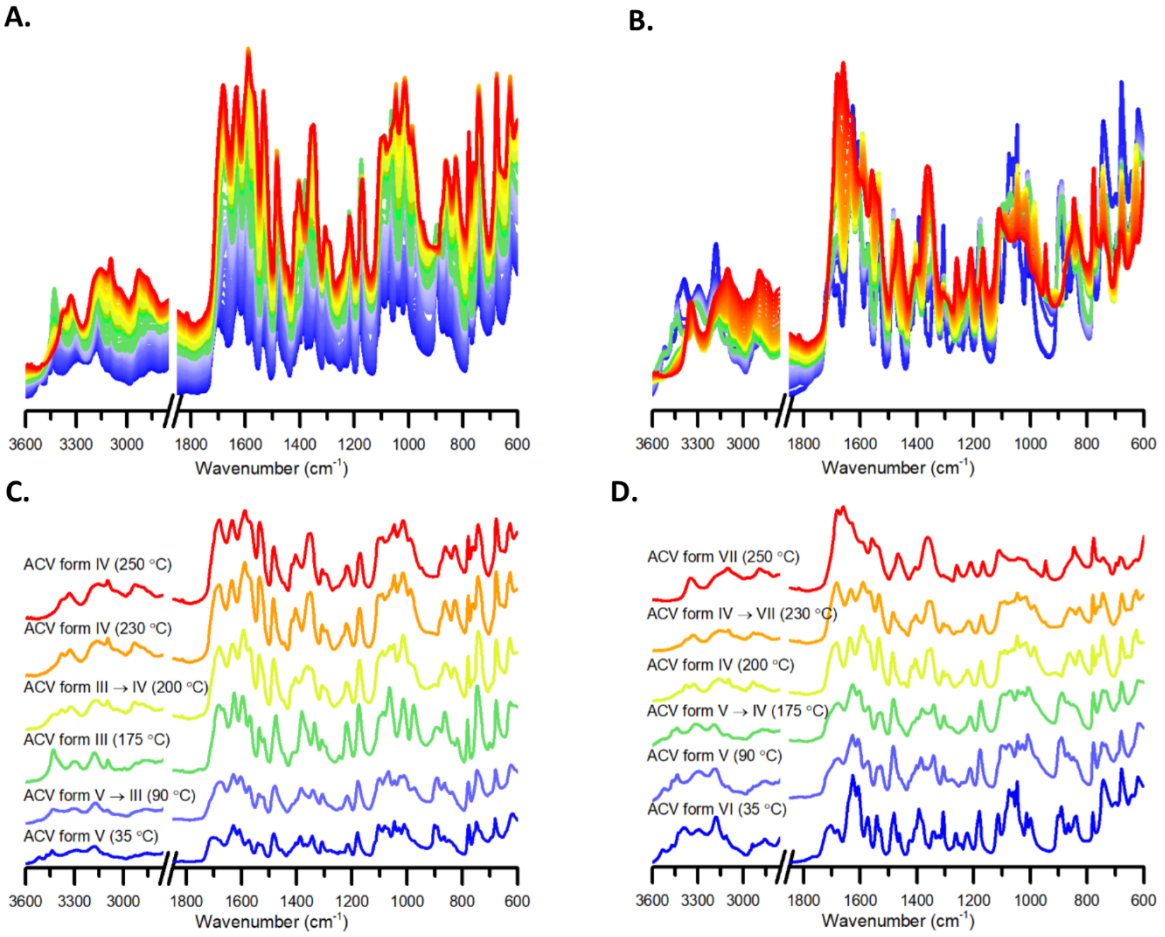

Figure S 16. Variable temperature FTIR spectra of ACV form V (A and C) and ACV form VI (B and D) recorded in the temperature range from 30 to 250 °C.

Section S9. Solvent induced phase transitions of ACV form V (3:2 ACV/water hydrate)

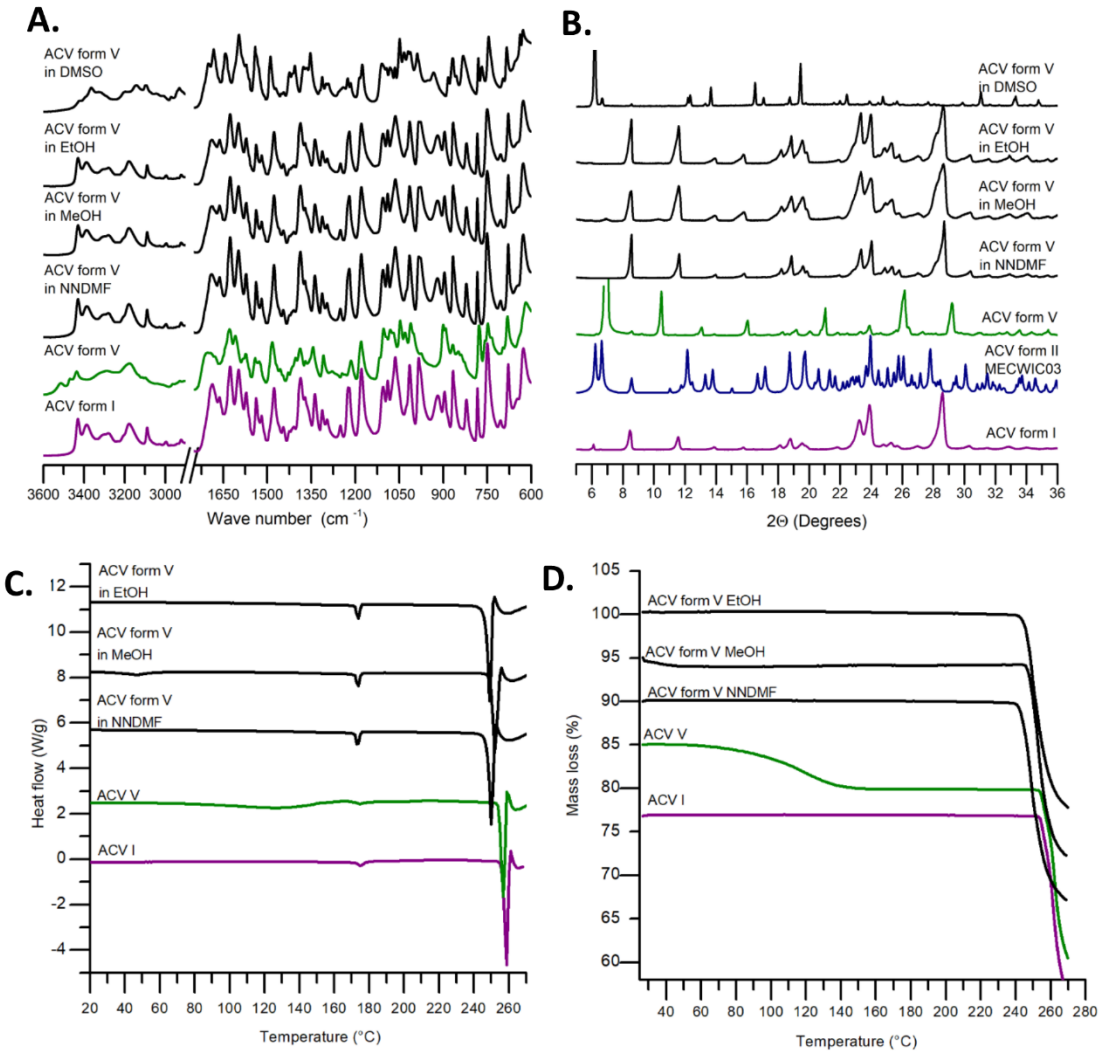

Figure S 17. FTIR spectra (A), PXRD patterns (B), DSC (C) and TGA (D) thermograms of ACV form V in methanol, ethanol and N,N-dimethylformamide after 4 weeks of slurring.

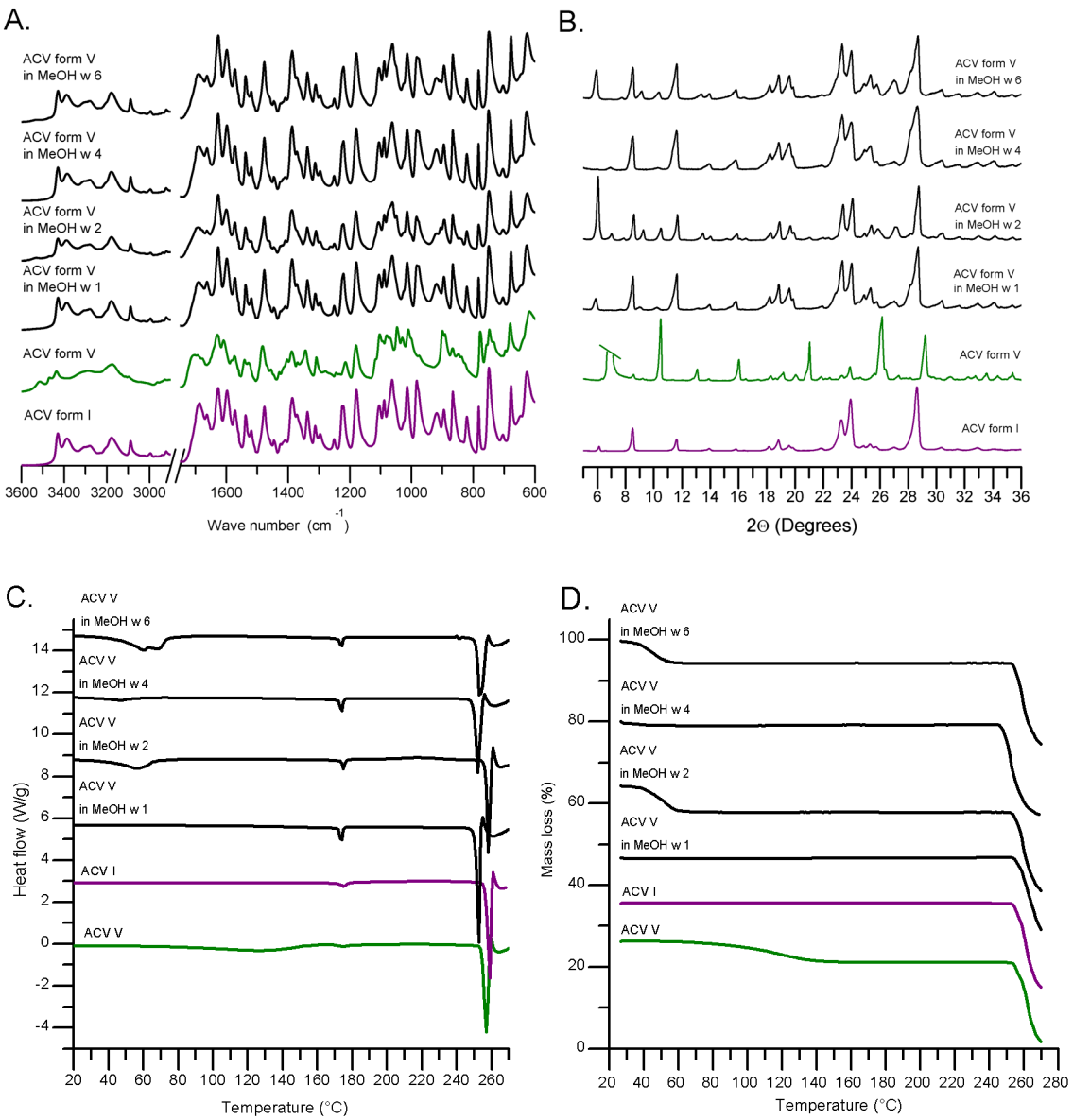

Figure S 18. FTIR spectra (A) and PXRD patterns (B) of ACV form V slurried in methanol after 1, 2, 4 and 6 weeks.

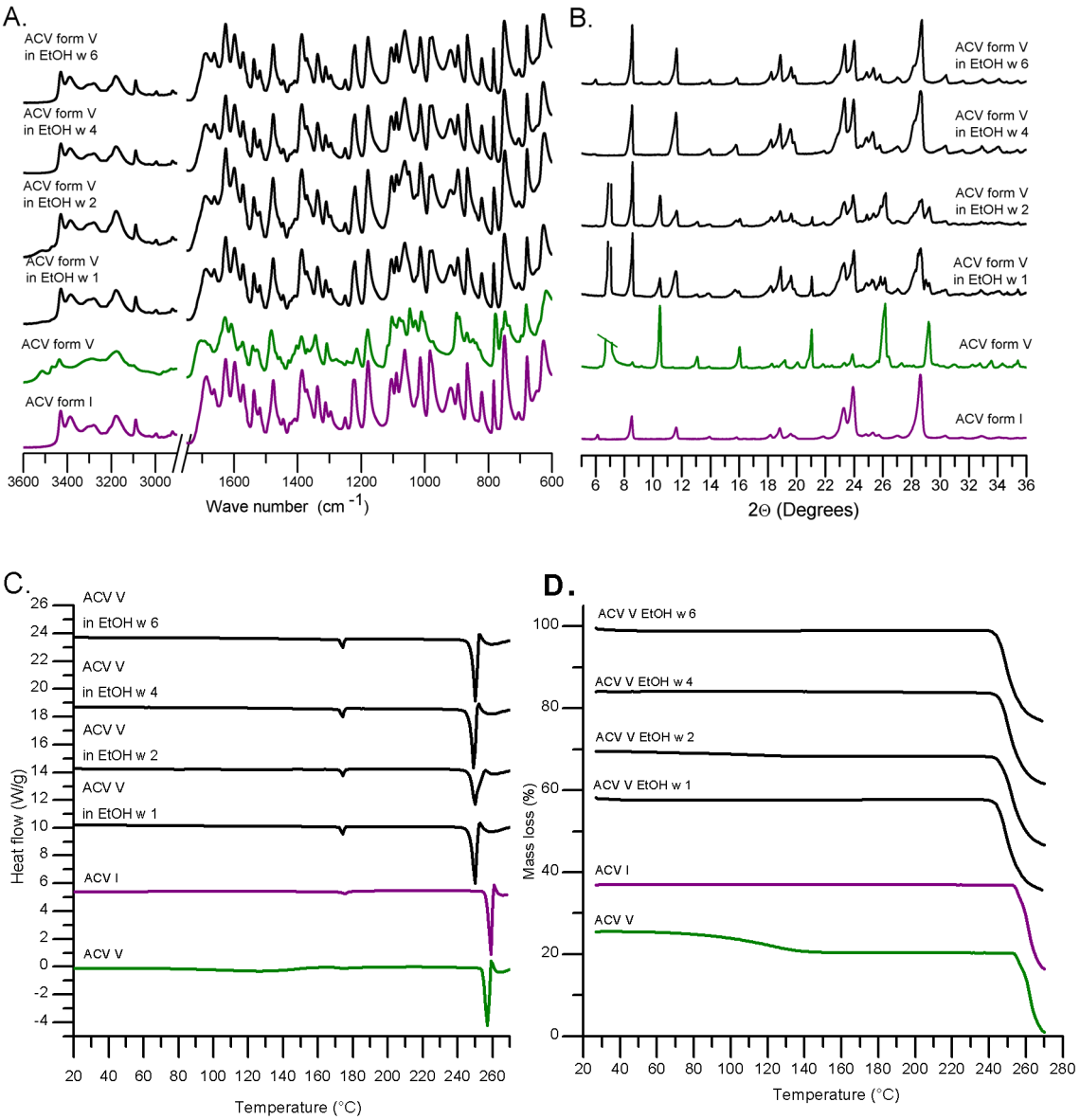

Figure S 19. FTIR spectra (A), PXRD patterns (B), DSC (C) and TGA thermograms of ACV form V in ethanol after 1, 2, 4 and 6 weeks.

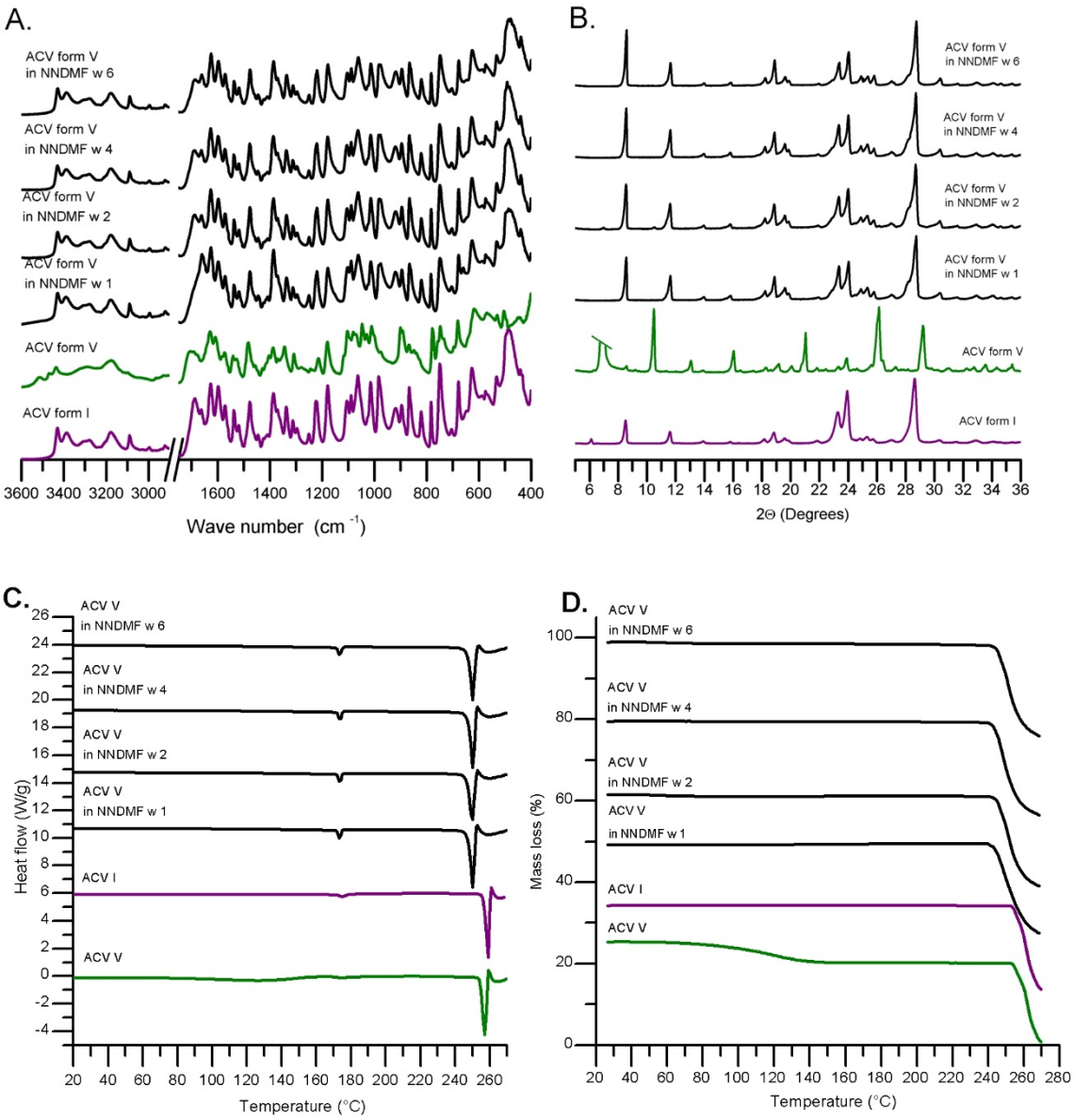

Figure S 20. FTIR spectra (A), PXRD patterns (B), DSC (C) and TGA (D) thermograms of ACV form V in N,N-dimethylformamide after 1, 2, 4 and 6 weeks.

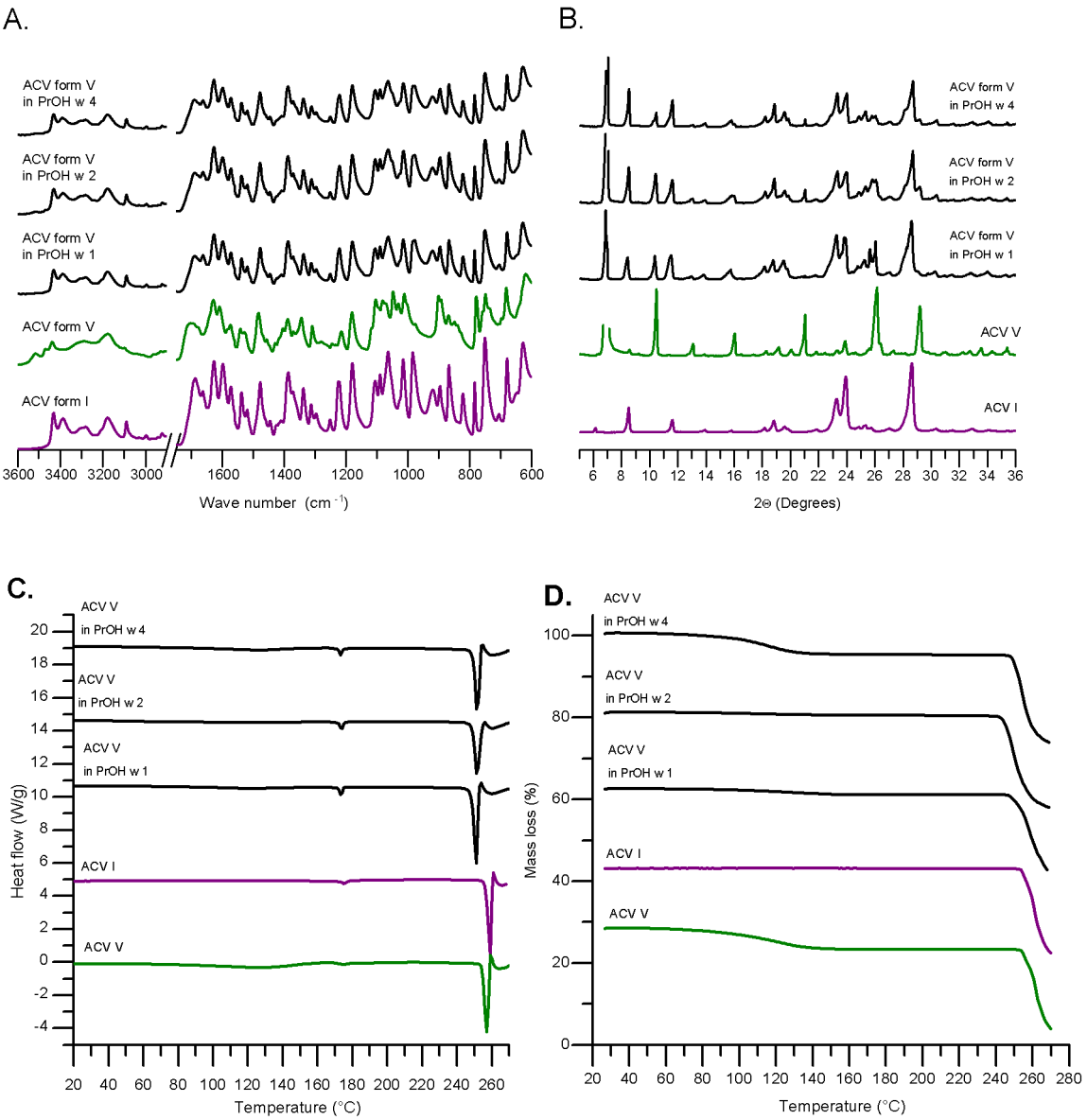

Figure S 21. FTIR spectra (A), PXRD patterns (B), DSC (C) and TGA (D) thermograms of ACV form V in propanol after 1, 2 and 4 weeks of storage.

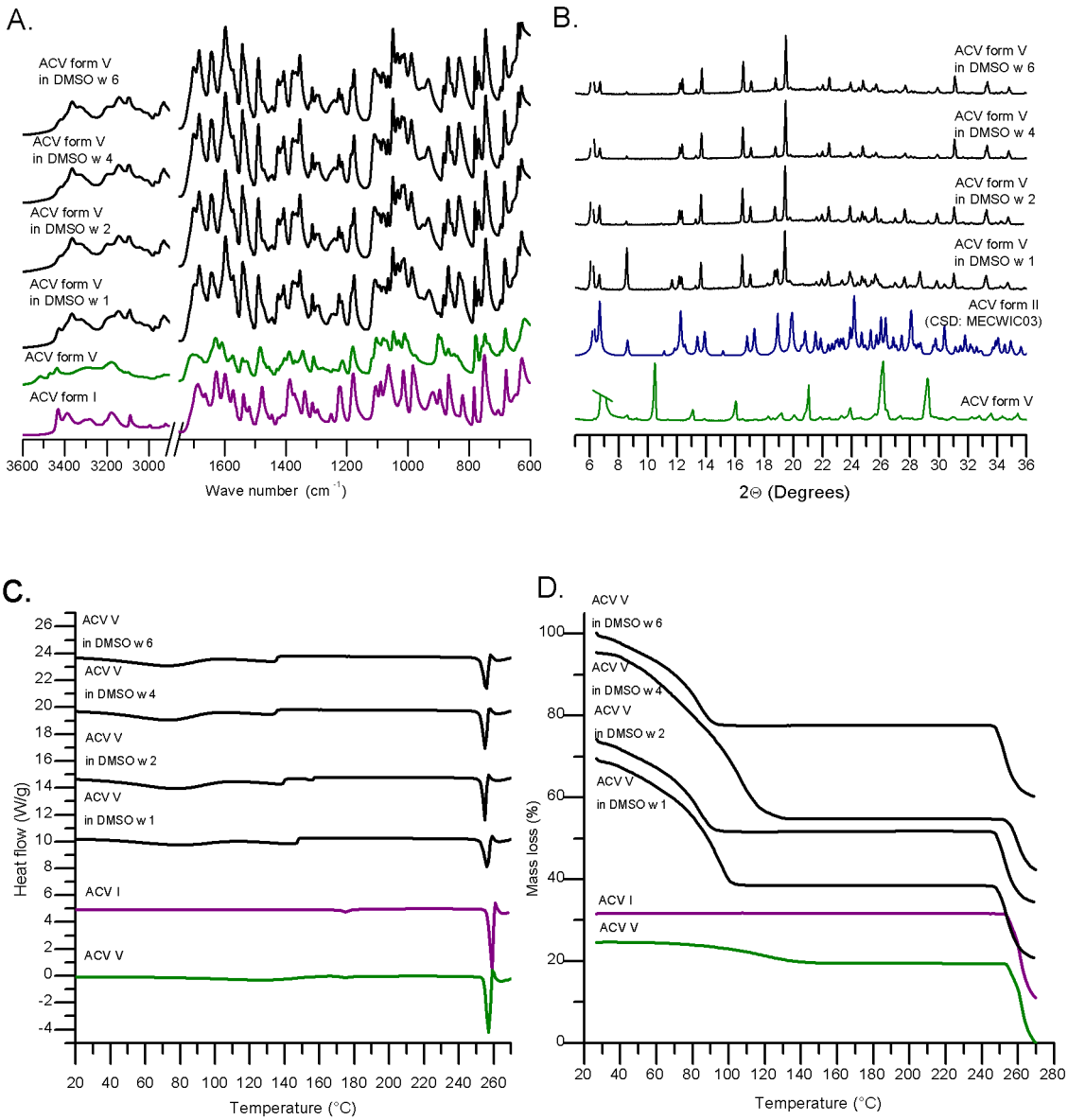

Figure S 22. FTIR spectra (A) and PXRD patterns (B) of ACV form V in dimethyl sulfoxide after 1, 2, 4 and 6 weeks. The observed mass loss in the TGA and endothermal event recorded in the DSC in the temperature range below 180 °C are due to evaporation of DMSO from gel-like form II.

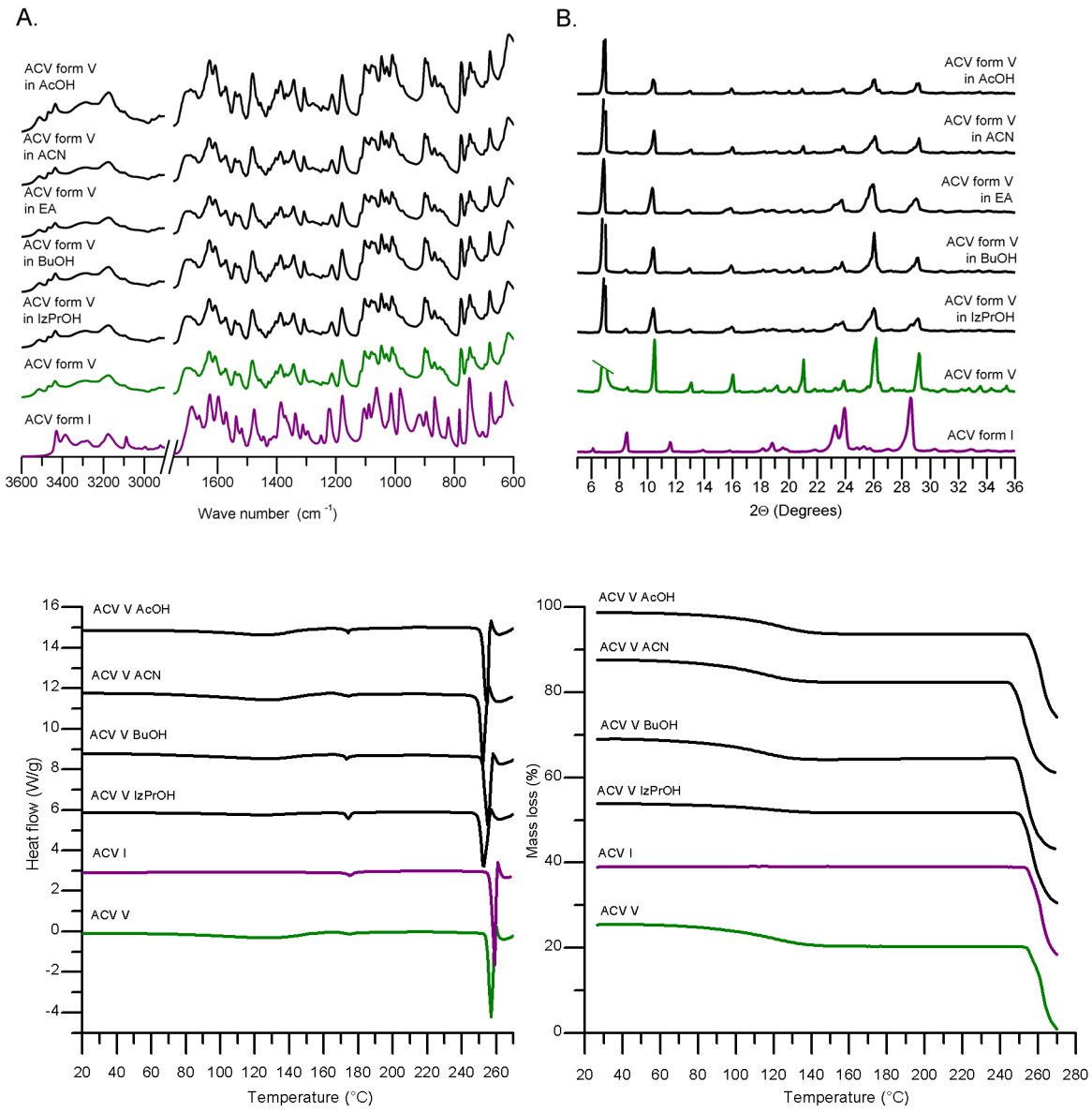

Figure S 23. FTIR spectra (A), PXRD patterns (B), DSC (C) and TGA (D) thermograms of ACV form V slurried in acetic acid, acetonitrile, acetone, butanol and isopropanol for four weeks.

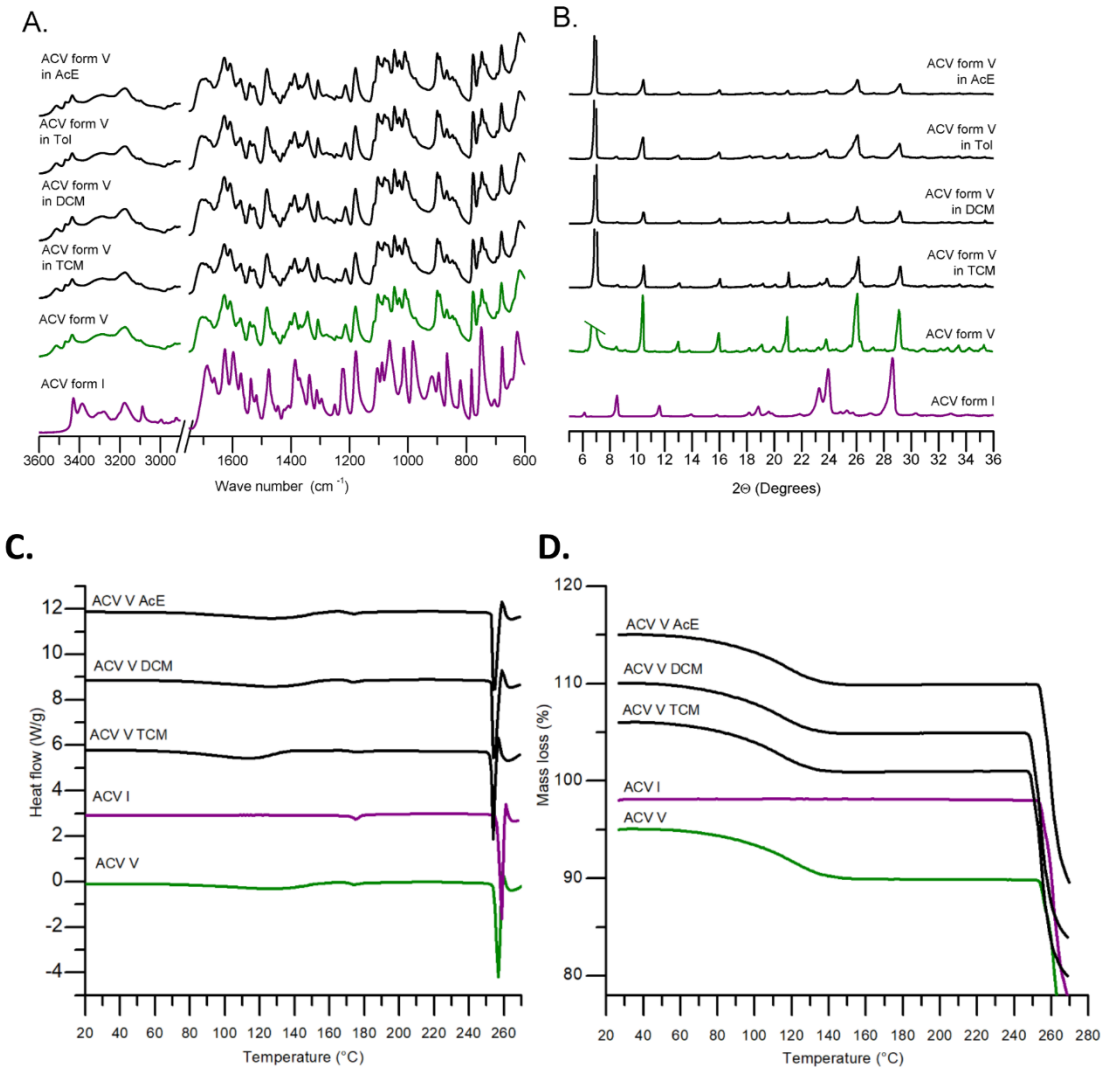

Figure S 24. FTIR spectra (A) and PXRD patterns (B), DSC (C) and TGA (D) thermograms of ACV form V in ethyl acetate, toluene, dichloromethane and trichloromethane after four weeks of storage.

Section S10. Solvent induced phase transitions of ACV form I (anhydrous form I)

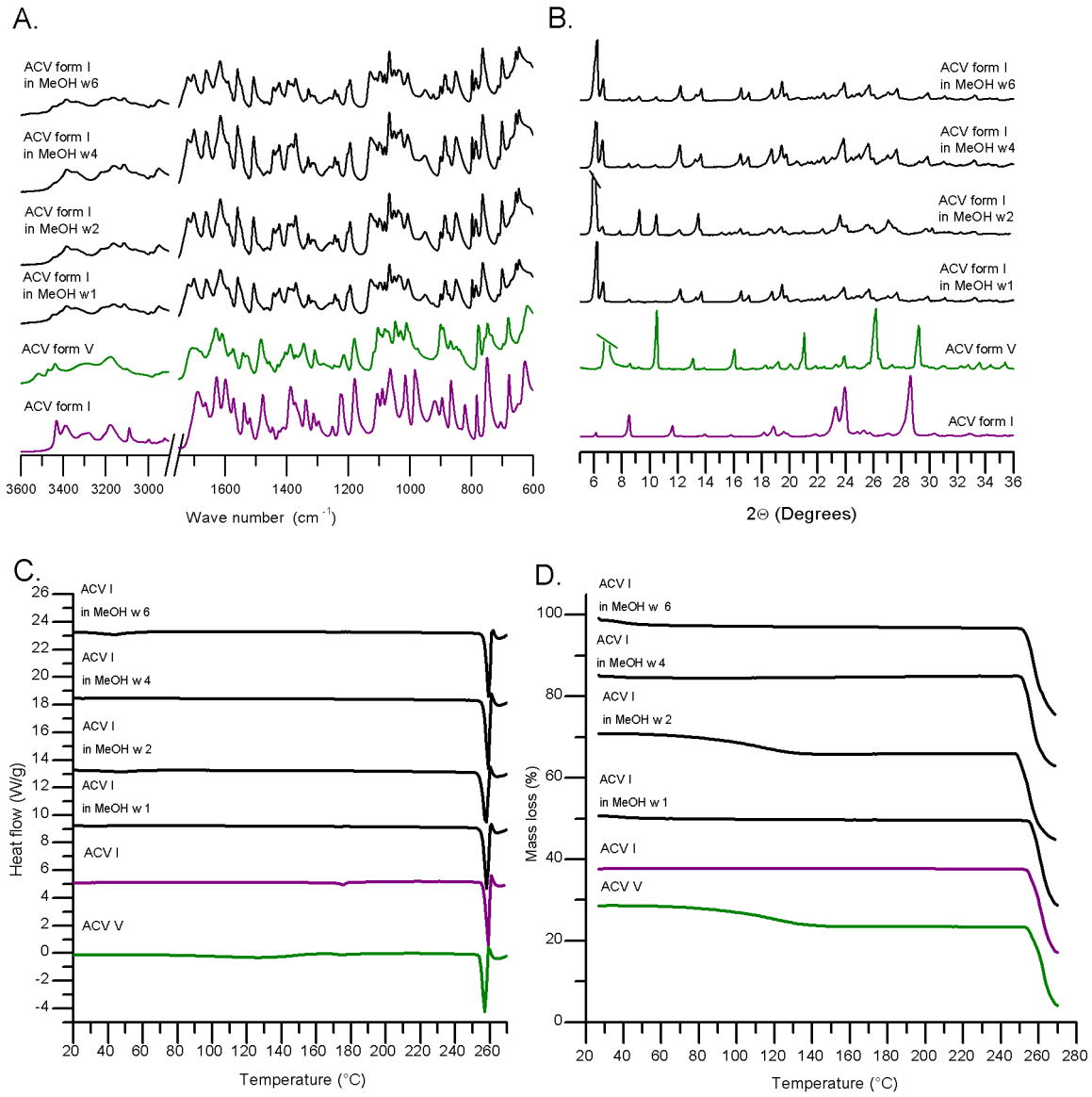

Figure S 25. FTIR spectra (A), PXRD patterns (B), DSC (C) and TGA (D) thermograms of ACV form I slurried in methanol after 1, 2, 4 and 6 weeks of storage.

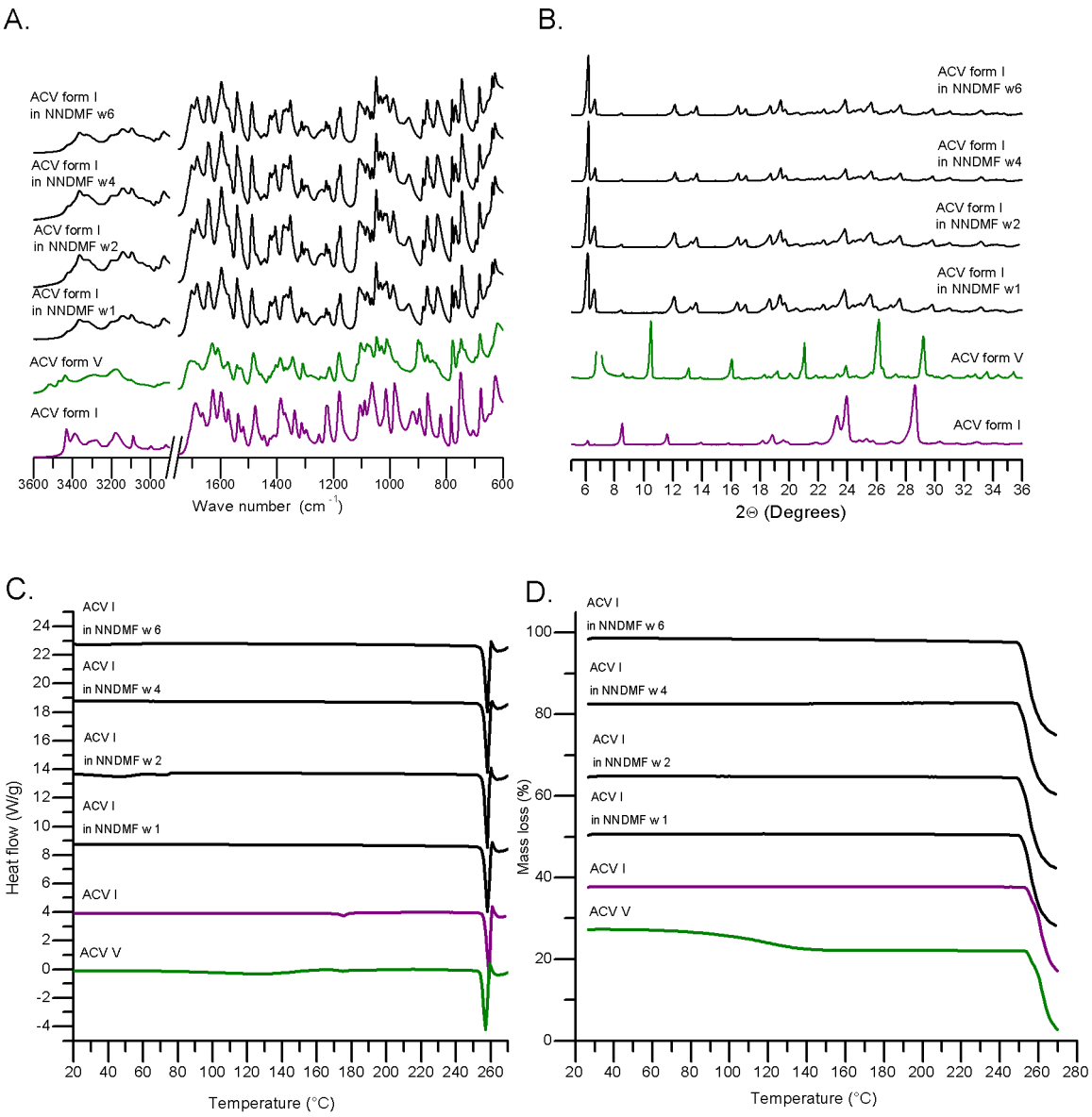

Figure S 26. FTIR spectra (A), PXRD patterns (B), DSC (C) and TGA (D) thermograms of ACV form I slurried in N,N-dimethylformamide after 1, 2, 4 and 6 weeks of storage.

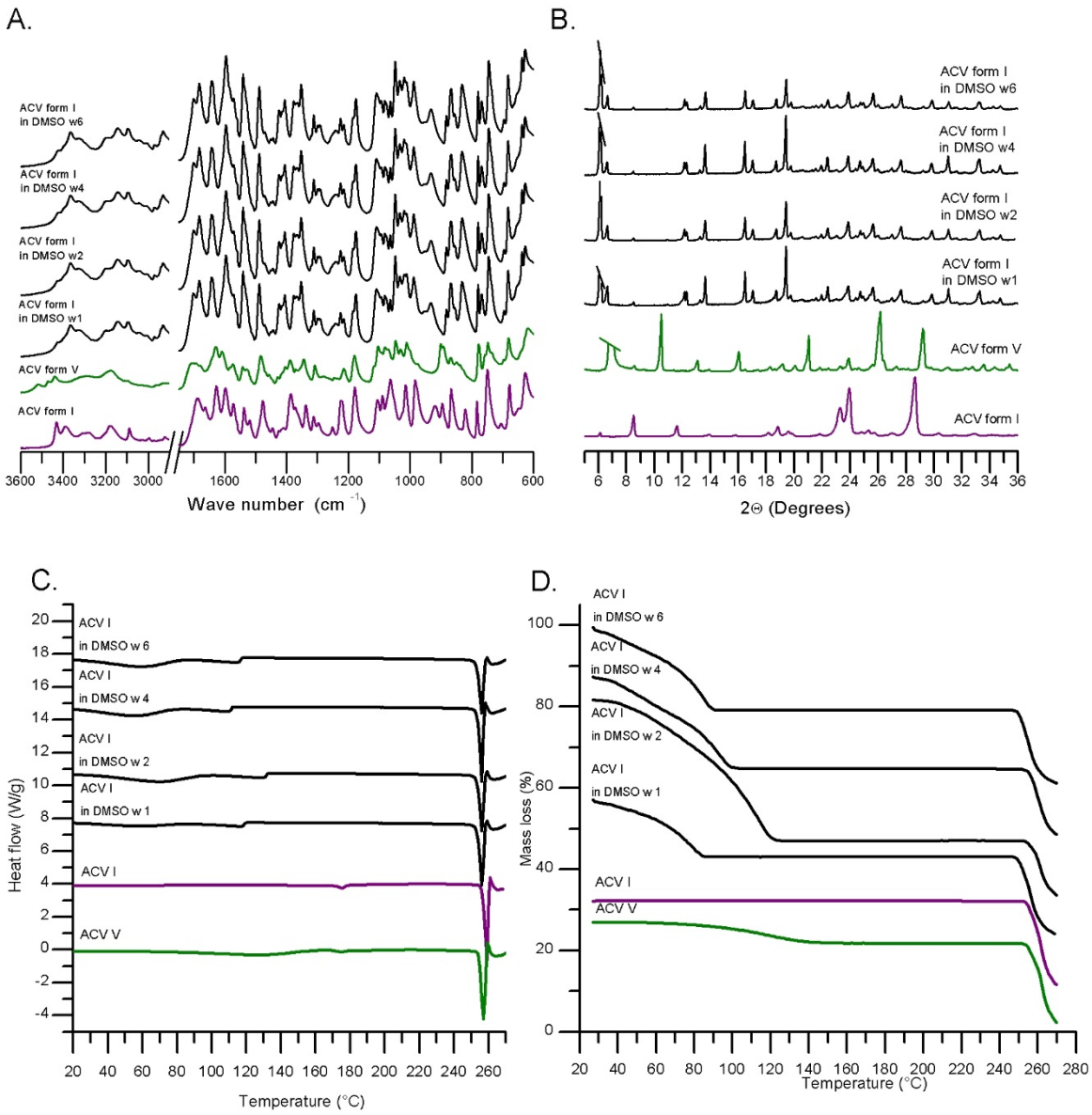

Figure S 27. FTIR spectra (A), PXRD patterns (B), DSC (C) and TGA (D) thermograms of ACV form I slurried in dimethyl sulfoxide after 1, 2, 4 and 6 weeks of storage. The observed mass loss in the TGA and endothermal event recorded in the DSC in the temperature range below 180 °C are due to evaporation of DMSO from gel-like form II.

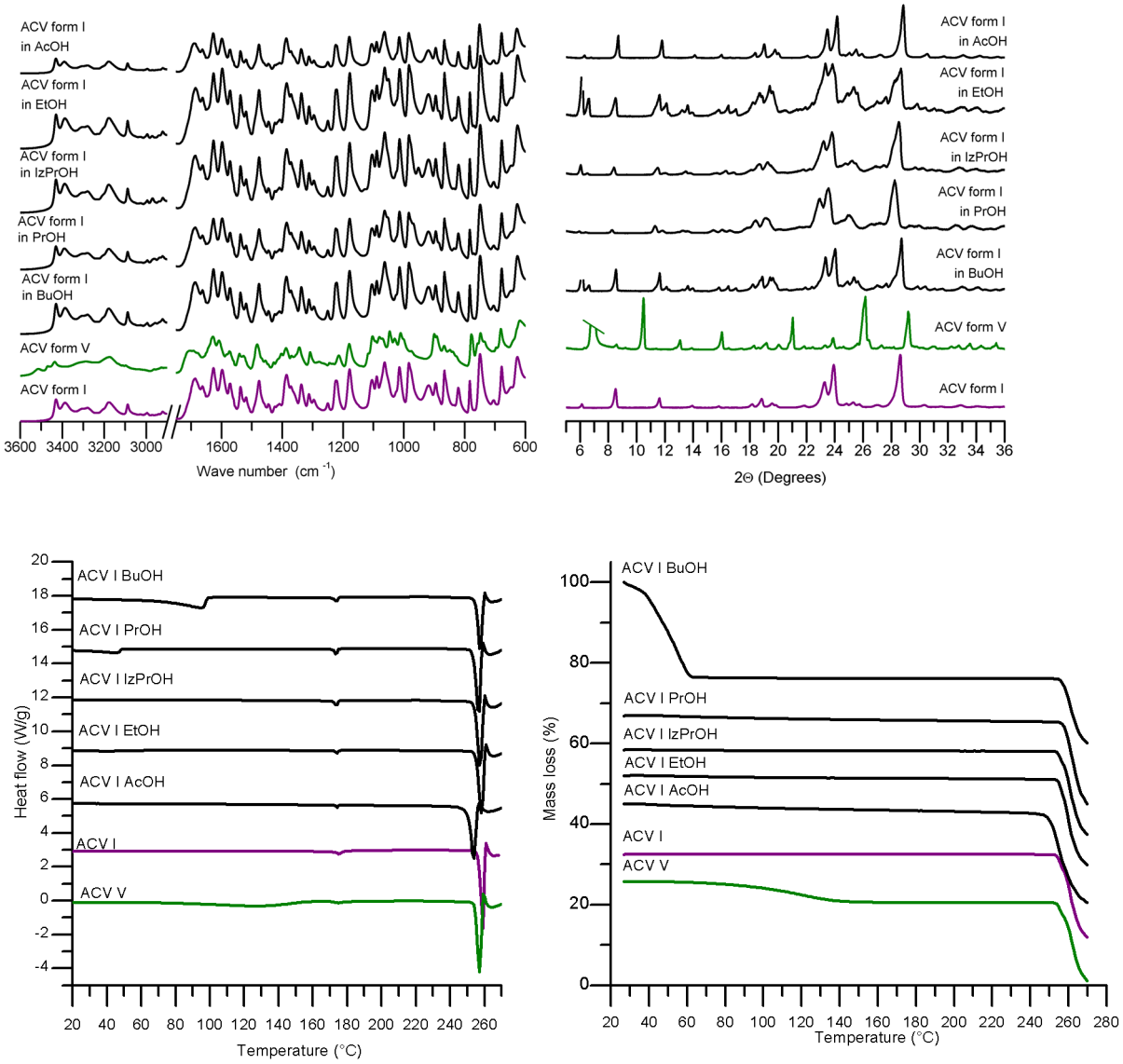

Figure S 28. FTIR spectra (A), PXRD patterns (B), DSC (C) and TGA (D) thermograms of ACV form I in butanol, propanol, isopropanol, ethanol and acetic acid after four weeks of slurring.

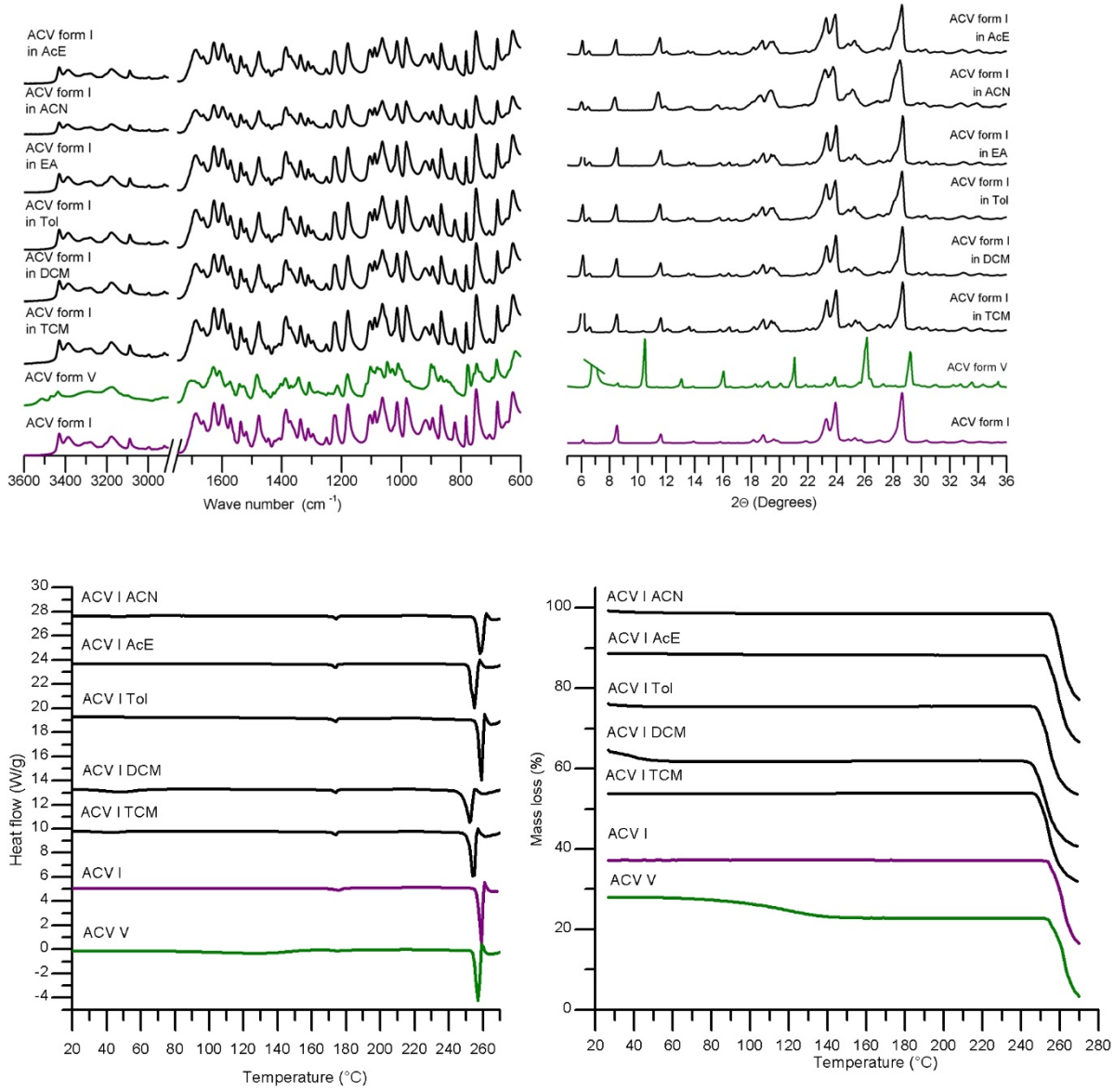

Figure S 29. FTIR spectra (A), PXRD patterns (B), DSC (C) and TGA (D) thermograms of ACV form I in ethyl acetate, acetonitrile, acetone, toluene, dichloromethane and trichloromethane after four weeks of slurring.